

NASA/CR—2008-215280



# Gelation in Aerosols; Non-Mean-Field Aggregation and Kinetics

*C.M. Sorensen and A. Chakrabarti*  
*Kansas State University, Manhattan, Kansas*

---

August 2008

## NASA STI Program . . . in Profile

Since its founding, NASA has been dedicated to the advancement of aeronautics and space science. The NASA Scientific and Technical Information (STI) program plays a key part in helping NASA maintain this important role.

The NASA STI Program operates under the auspices of the Agency Chief Information Officer. It collects, organizes, provides for archiving, and disseminates NASA's STI. The NASA STI program provides access to the NASA Aeronautics and Space Database and its public interface, the NASA Technical Reports Server, thus providing one of the largest collections of aeronautical and space science STI in the world. Results are published in both non-NASA channels and by NASA in the NASA STI Report Series, which includes the following report types:

- **TECHNICAL PUBLICATION.** Reports of completed research or a major significant phase of research that present the results of NASA programs and include extensive data or theoretical analysis. Includes compilations of significant scientific and technical data and information deemed to be of continuing reference value. NASA counterpart of peer-reviewed formal professional papers but has less stringent limitations on manuscript length and extent of graphic presentations.
- **TECHNICAL MEMORANDUM.** Scientific and technical findings that are preliminary or of specialized interest, e.g., quick release reports, working papers, and bibliographies that contain minimal annotation. Does not contain extensive analysis.
- **CONTRACTOR REPORT.** Scientific and technical findings by NASA-sponsored contractors and grantees.
- **CONFERENCE PUBLICATION.** Collected

papers from scientific and technical conferences, symposia, seminars, or other meetings sponsored or cosponsored by NASA.

- **SPECIAL PUBLICATION.** Scientific, technical, or historical information from NASA programs, projects, and missions, often concerned with subjects having substantial public interest.
- **TECHNICAL TRANSLATION.** English-language translations of foreign scientific and technical material pertinent to NASA's mission.

Specialized services also include creating custom thesauri, building customized databases, organizing and publishing research results.

For more information about the NASA STI program, see the following:

- Access the NASA STI program home page at <http://www.sti.nasa.gov>
- E-mail your question via the Internet to [help@sti.nasa.gov](mailto:help@sti.nasa.gov)
- Fax your question to the NASA STI Help Desk at 301-621-0134
- Telephone the NASA STI Help Desk at 301-621-0390
- Write to:  
NASA Center for AeroSpace Information (CASI)  
7115 Standard Drive  
Hanover, MD 21076-1320

NASA/CR—2008-215280



# Gelation in Aerosols; Non-Mean-Field Aggregation and Kinetics

*C.M. Sorensen and A. Chakrabarti*  
*Kansas State University, Manhattan, Kansas*

Prepared under Grants NAG3-2360 and NNC04GA746

National Aeronautics and  
Space Administration

Glenn Research Center  
Cleveland, Ohio 44135

---

August 2008

*Level of Review:* This material has been technically reviewed by NASA technical management.

Available from

NASA Center for Aerospace Information  
7115 Standard Drive  
Hanover, MD 21076-1320

National Technical Information Service  
5285 Port Royal Road  
Springfield, VA 22161

Available electronically at <http://gltrs.grc.nasa.gov>

# Gelation in Aerosols; Non-Mean-Field Aggregation and Kinetics

C.M. Sorensen and A. Chakrabarti  
Kansas State University  
Manhattan, Kansas 66506

## Abstract

Nature has many examples of systems of particles suspended in a fluid phase; colloids when in a liquid, aerosols when in a gas. These systems are inherently unstable since if the particles can come together, van der Waals forces will keep them together. In this work we studied the aggregation kinetics of particulate systems, most often aerosols. The emphasis of our work was to study dense systems and systems that gel since previous work had not considered these. Our work obtained a number of significant discoveries and results.

1. We found it useful to define three regimes of aggregation based on the relative distance between clusters: the *cluster dilute* regime where the nearest neighbor separation is very large compared to the cluster size, the *intermediate* regime where the nearest neighbor separation becomes comparable to the cluster size, and the *cluster dense* regime where the nearest neighbor separation is so small that the clusters travel with a nondiffusive, straight line motion between collisions. Previous work had concerned only the cluster dilute regime.
2. We found that the mean field description of aggregation continues to work well as the system evolves into the intermediate and dense regimes.
3. We found that aggregation in the cluster dense regime leads to the formation of superaggregates, i.e., aggregates with a fractal dimension of 2.6 over large length scales made up of smaller aggregates with a fractal dimension of 1.8 over their smaller length scales. Such superaggregates were found in the soot from combustion of heavily sooting fuels.
4. The kinetics crosses over from the well known dilute case to the intermediate and dense cases as identified by an increasing aggregation kernel homogeneity.
5. These results above allow us to describe gelation as the evolution of a particulate system from cluster dilute through the intermediate regime to the cluster dense where the system ultimately gels.
6. Based on our understanding of gelation we, for the first time, caused an aerosol to gel. These aerosol gels have unique properties and a patent has been filed.
7. Simulation of charged aerosol aggregation showed that the presence of a small fraction (10% or less) of charged monomers does not yield significant differences in the growth kinetics.
8. We also studied how light scatters from these aggregates relative to scattering from simple spheres. We did this because our experiments use light scattering to probe the systems. We found heretofore undescribed patterns in the scattering as a function of angle which give insight into the nature of the scattering process. We also studied multiple scattering in dense particulate systems.

## Superaggregates in Dense Particulate Systems

### Flames

We have shown that soot formed in laminar diffusion flames of heavily sooting fuels evolves through four distinct growth stages which give rise to four distinct aggregate fractal morphologies. Each successive stage grows upon the previous stage; hence aggregates of one morphology, parameterized by a fractal dimension, form larger superaggregates or gels of a different morphology with a different fractal dimension. These results were inferred from large and small angle static light scattering from the flames,

microphotography of the flames, and analysis of soot sampled from the flames. These results and the analysis were substantiated by comparison to computer simulations. The growth stages occur approximately over four successive orders of magnitude in aggregate size and involve either diffusion limited cluster aggregation or percolation in either three or two dimensions. Table 1 gives an overview of our results, figures 1 to 4 show examples.

TABLE 1.—THE REALM OF SUPERSOOT

<u>Stage 1</u>	<u>Stage 2</u>	<u>Stage 3</u>	<u>Stage 4</u>
DLCA	percolation or restructuring?	2d, DLCA	2d percolation?
$D \approx 1.8$	$D \approx 2.6$	$D \approx 1.4$	$D = 1.9$
aggregates	superagg(SA)	supersuperagg(SSA)	gel network
$\sim 1 \mu\text{m}$	$\sim 20 \mu\text{m}$	$\sim 200 \mu\text{m}$	

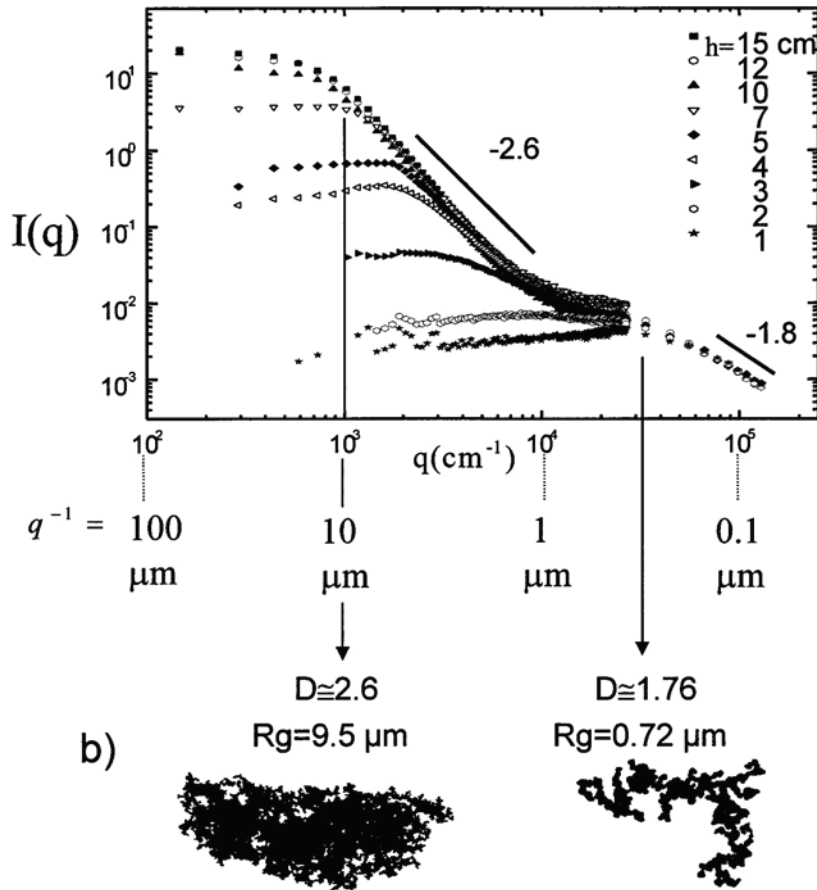


Figure 1.—Light scattering showing both the  $D = 2.6$  and  $1.8$  morphologies, stage 2 and 1, of soot superaggregates in an acetylene/air diffusion flame. Also shown are soot aggregates extracted from the flame with these morphologies.

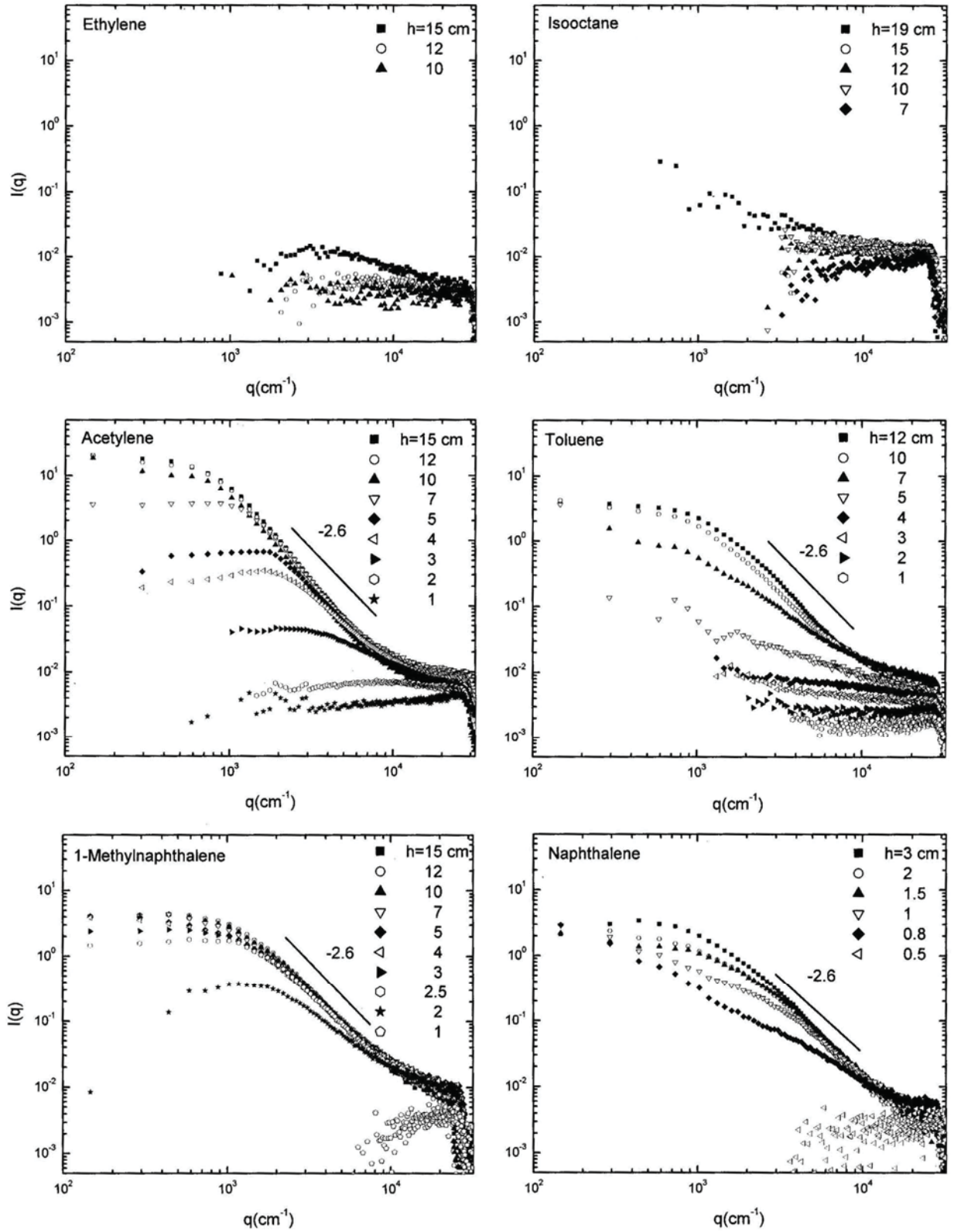


Figure 2.—Light scattering from a variety of flames some of which do not show superaggregates, some do.

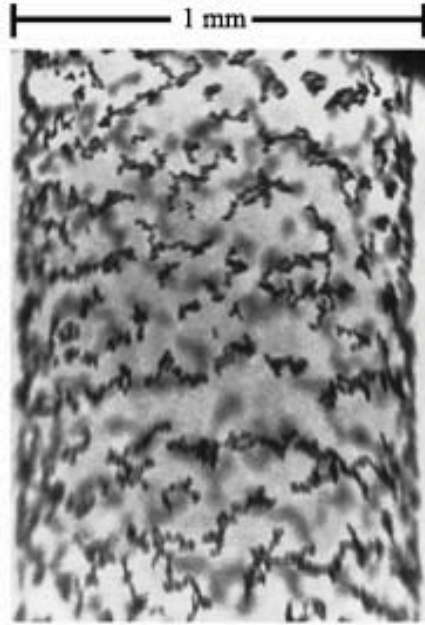


Figure 3.—Example of 2-D stage 3 soot.



Figure 4.—Example of stage 4, continuous 2-D percolation, soot.

### Simulations

These results can be understood with the aid of our simulations of off-lattice cluster-cluster aggregation for diffusion-limited (DLCA), ballistic-limited, and reaction-limited cluster aggregation classes. We find that as the system evolves and becomes dense, the largest cluster develops a hybrid structure with mass fractal dimension  $D_f = 2.6$  over large length scales, while at smaller length scales, the early time dilute-limit fractal structure with  $D = 1.8$  is frozen in, figure 5. Consistent with our experiments the largest cluster is thus an aggregate of smaller aggregates with a different fractal dimension, and we call it a “superaggregate.” The crossover length separating the two morphologies, which we call the critical radius of gyration, can be calculated based on a simple theory that assumes a monodisperse cluster size distribution. This agrees well with simulation results for DLCA.

### Chamber Explosions

We use 4 and 17 liter chambers (fig. 6) to create dense, nanoparticle aerosols which will gel. The dense aerosol is created by rapid (explosive) reaction of gases such as  $C_2H_2$  or  $SiH_4$  with an oxidizer (e.g.,  $O_2$ ). From digitized pictures of soot clusters formed after the explosion of a hydrocarbon gas mixed with oxygen, the cluster morphology was determined by two different methods: structure factor and perimeter analysis. Here again we found a hybrid, superaggregate morphology characterized by a fractal dimension of  $D \approx 1.8$  between the monomer size, ca. 50 nm, and 1  $\mu m$  and  $D \approx 2.6$  at larger length scales up to  $\sim 10 \mu m$ . The superaggregate morphology is a consequence of late stage aggregation in a cluster dense regime near a gel point.

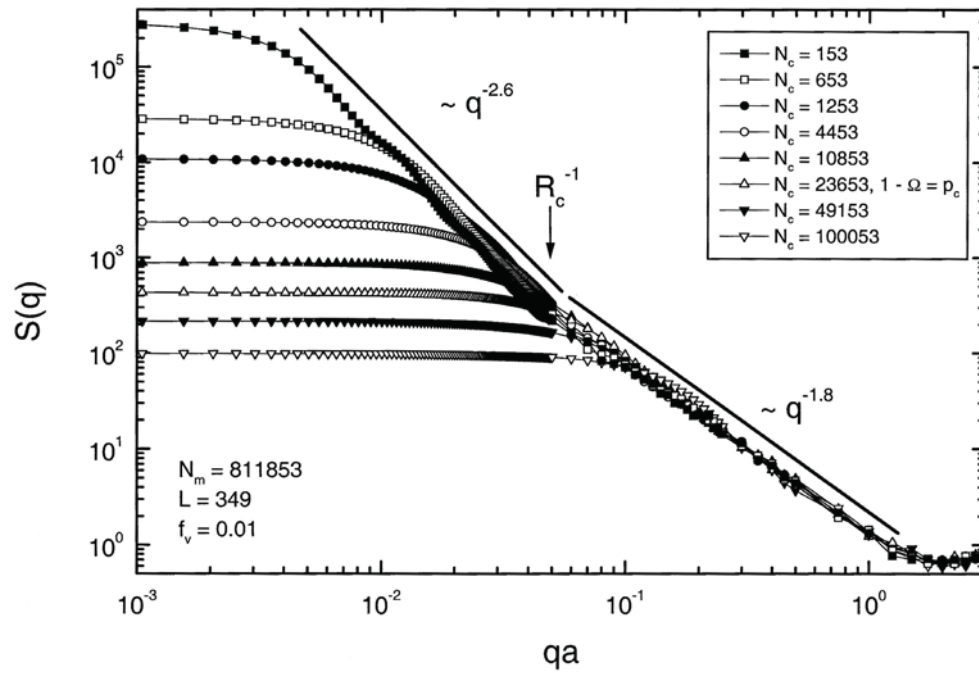


Figure 5.—Structure factor, hence expected light scattering pattern, of 3-D simulations of aggregation. Late in the run both  $D = 1.8$  and  $2.6$  morphologies appear.



Figure 6.—A 17 liter chamber in which carbon aerosol is gelled.

## Aerosol Gels

Using the chamber explosions, we discovered a novel one-step method to produce aerogel-like porous materials. This method involves the gelation of nanoparticles (primary particles) in the aerosol phase to create a material that we have named an *aerosol gel*. So far we have made both carbon aerosol gels (fig. 7) and silica ( $\text{SiO}_2$ ) aerosol gels (fig. 8). However, any collection of finely divided primary particles with large enough volume fraction can produce an aerosol gel when allowed to aggregate regardless of the chemical composition of the parent primary particles. In the case of the carbon aerosol gel the initial aerosol is composed of nanometer sized carbon particles produced rapidly by exploding any one of a number of hydrocarbons with oxygen in a closed chamber. This method of making an aerosol gel is not a wet process and does not require a catalysis. Furthermore, the most important advantage of this method is the non-requirement of the supercritical drying step. The carbon aerosol gels have properties quite comparable to those of the carbon aerogels. The carbon aerosol gels have high specific area of about  $400 \text{ m}^2/\text{g}$  and an extremely low density as low as  $2.5 \text{ mg/cc}$ . These materials also have high electrical conductivity and highly crystalline primary particles. This carbon aerosol gel is significantly different than ordinary carbon black and soot formed as byproduct during combustion of any hydrocarbon fuel; it is a new material.

The silica aerosol gel has specific surface areas of ca.  $500 \text{ m}^2/\text{g}$ . It can be made either hydrophilic or hydrophobic depending on the oxidizer used during its synthesis or post gel surface treatment (fig. 9).



Figure 7.—Carbon aerosol gel.



Figure 8.—Silica aerosol gel.



Figure 9.—Carbon coated silica aerosol gel with water drop to demonstrate superhydrophobicity.

## Aggregation Kinetics

### Simulations

Cluster-Cluster aggregation has been studied in our work via large scale Monte Carlo simulations for diffusion-limited (DLCA), ballistic-limited (BLCA), and reaction-limited (RLCA) cluster aggregation classes in 3-D. We investigated the growth kinetics for systems which evolve from a dilute to a dense state, a state we have name “cluster dense,” and then ultimately gel. We studied over three orders of magnitude in monomer volume fraction  $f_v$ . DLCA model results show a power law growth kinetics with growth accelerating as the volume fraction occupied by clusters increases with time and the system becomes dense. We found that only a weak spatial correlation develops among clusters when dense, and cluster-cluster correlation is not sufficient to explain the late time enhancement of the growth kinetics. Instead, both exponents,  $z$  and  $\lambda$ , characterizing the kinetics and size distribution, respectively, show universal functionality with cluster volume fraction, independent of the initial monomer volume fraction. Remarkably, the relationship between  $z$  and  $\lambda$  maintains its mean-field nature in 3-D. Results for the BLCA model in 3-D is quite similar to the DLCA model while the 3-D RLCA model shows an early time exponential growth that crosses over to a power law growth at late times when the system becomes dense.

We have also studied an off-lattice Monte Carlo simulation of DNA-mediated colloidal assembly. In this simulation, aggregation-fragmentation of a binary mixture of DNA-coated colloidal particles is studied through a simplified model of base-pair hybridization. Bonding between monomers is modeled as a simple temperature sensitive A/B type interaction, where type A and B monomers can only bond to the opposite type (no A/A or B/B attachments are allowed). The actual chemistry of base-pair hybridization is not included in the model. The morphological structures of the clusters formed as well as the kinetics of growth are analyzed in our 2-D simulations. The fractal dimension and kinetic growth exponents for clusters formed near the DNA “melting” temperature agree with those seen previously for 2-D diffusion-limited cluster aggregation (DLCA) models. The clusters appear more compact, exhibiting signs of local order at intermediate temperature values. At higher temperatures, formation of large clusters is not favorable under the action of temperature-dependent fragmentation and the system eventually reaches a steady state as a collection of small aggregates. The temperature profile for this *dissolution* of the colloidal assembly is sharp, indicating that the selective hybridization process provides a highly sensitive measurement tool. At high temperatures, we analyze the steady state behavior of the average cluster size in terms of an aggregation-fragmentation model.

### Soot Aerosol Aggregation up to Gelation

We studied the kinetics, morphology and structure of the quickly aggregating carbon soot particles rapidly produced during the explosion of a mixture of a hydrocarbon gas and oxygen inside a closed chamber. We used Small Angle Static Light Scattering (SASLS) technique to do this. Our device allows us to detect the scattered light in the angular range  $0.05^\circ \leq \theta \leq 15^\circ$ , which corresponds to  $q$  values in the range  $100 \text{ cm}^{-1} \leq q \leq 3 \times 10^{-4} \text{ cm}^{-1}$ .

We built a small and thin cylindrical disk combustion chamber with a circular glass window on both ends of the cylinder (fig. 10) for the purpose. The internal space of the chamber is 51 wide and 10 mm long. The chamber was first evacuated and then filled to different pressures with a hydrocarbon gas-oxygen mixture and then ignited using a spark plug. Then the laser light gets scattered by the soot aggregates inside the chamber.

One typical example of the measured scattered light intensity from our small angle SLS device plotted versus  $q$  is presented in figure 11. The structure factor analysis of the scattered light intensity revealed the fractal dimension to be  $1.55 \pm 0.05$ .

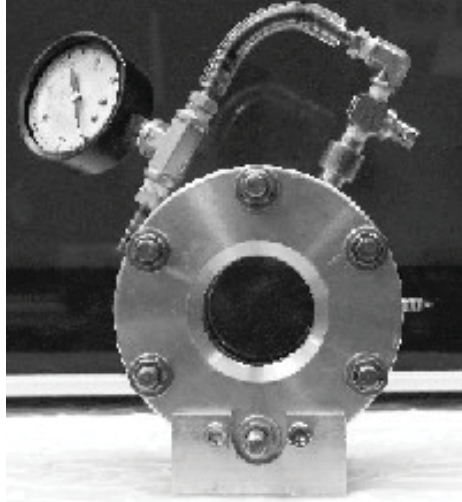


Figure 10.—Small chamber.

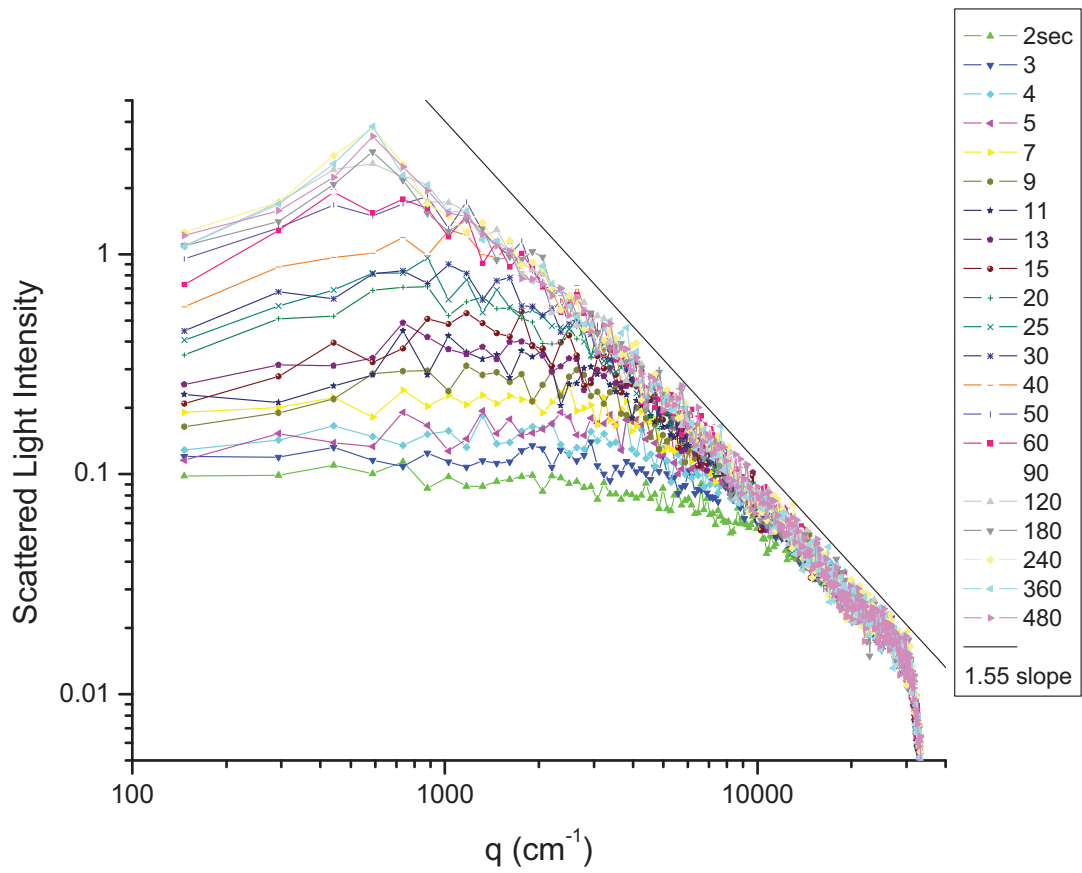


Figure 11.—Scattered Light Intensity versus  $q$  for initial absolute pressure 7 in. of Hg.

The Guinier analysis of the scattered light intensity yielded the ensemble average cluster size  $R_g$ . From  $R_g$  versus time we determined the aggregation kernel homogeneity and rate. These are shown in figures 12 and 13. Figure 12 shows the homogeneity increases with increasing volume fraction near the gel point. The limiting value of  $\lambda = 0.5$  is consistent with our simulations and theory.

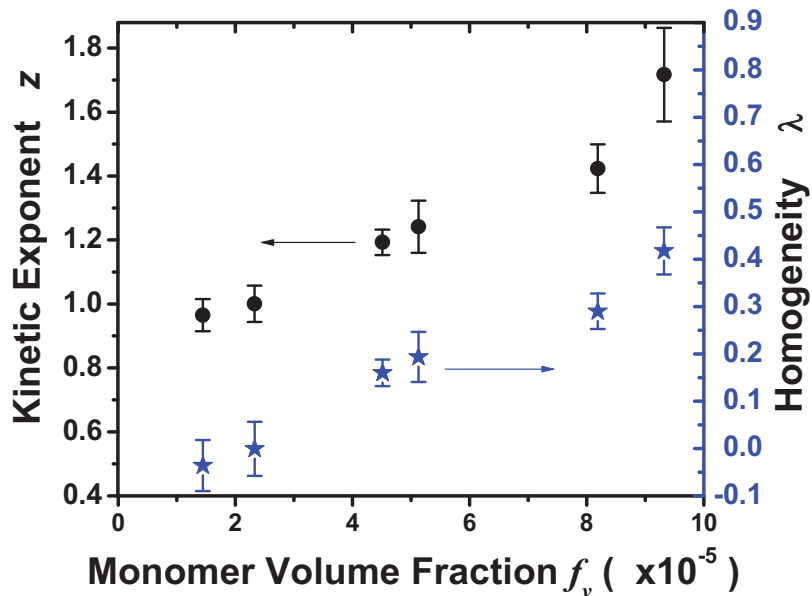


Figure 12.—A plot of the kinetic exponent  $z$  and the homogeneity  $\lambda$  versus the monomer volume fraction  $f_v$ . The enhanced aggregation kinetics with increasing  $f_v$  was the result of the effect of cluster crowding.

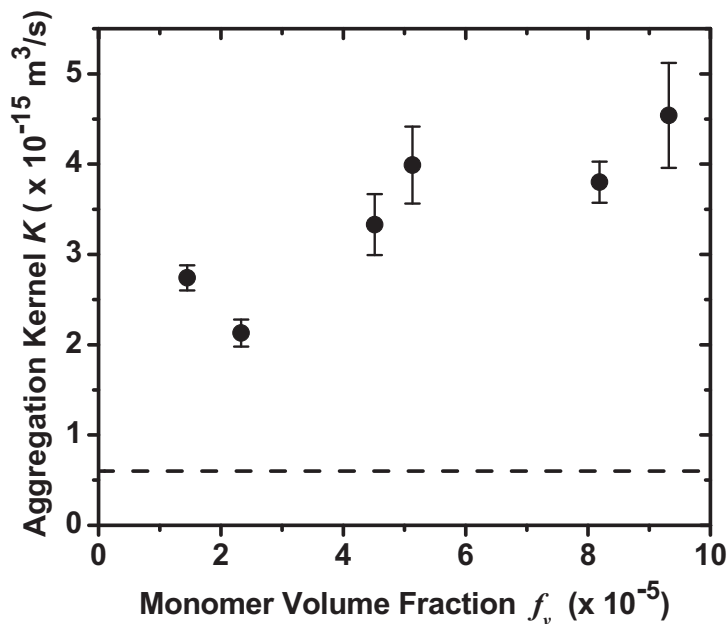


Figure 13.—A plot  $K(s_2, s_2)$  as a function of the monomer volume fraction  $f_v$ . The dashed line shows the theoretical value of  $K$  independent of the monomer volume fraction. The theoretical  $K$  was computed for a monodispersed aggregating system in continuum regime with Stokes-Einstein diffusion.

## Aggregation of Charged Aerosols

We studied the effect of placing charges on a certain fraction of the monomers in an aggregating aerosol system. This has relevance to planetary dusts, e.g., Mars, where solar UV photons will charge the dust particles via the photoelectric effect, and soot in flames. Maricq has studied the effect of charging on the aggregation of carbon soot in ethylene/air laminar diffusion flames. The charges are both positive and negative, producing a bipolar population. Due to aggregation, his experimental system eventually reaches a point at which the fraction of overall clusters with charges is ~33% positive and 33% negative.

Our study was done through the use of a Monte Carlo algorithm, modified from the standard DLCA/RLCA type to include a minimum image type coulomb interaction. The probability of a cluster move being accepted during a Monte Carlo time step is based on the Boltzmann factor  $B = \exp(-\Delta E)$ , where  $\Delta E$  is the difference in coulomb energy difference between the cluster before movement and after. The actual probability that a cluster is moved is  $B/(1+B)$ . Thus, for movements where the energy of the final state is significantly higher than the initial, the probability approaches 0. For movements where the energy of the final state is significantly lower than the initial, the probability approaches 1. When there is  $\sim 0$  change in energy, the movement probability is 0.5. Thus there is a deceleration in movements against the potential energy gradient and an acceleration in movements in the direction of the energy gradient.

Simulations were initially performed in the Epstein Regime, appropriate for rarified atmospheres, where the motion is still seen as diffusive, but the diffusion constant switches over from the continuum of  $D \sim R_g^{-1}$  to either  $D \sim R_g^{-2}$  or  $D \sim A^{-1}$ , where  $A$  is the cross sectional area of the cluster in the direction of cluster movement. Our first simulations were done with the latter, though comparison has been made between simulations using all the different diffusion constants.

For the purpose of our model, monomers are seen as nonconductive, meaning that the charge they initially possess is kept throughout the simulation. On aggregation with other monomers/clusters, the charges are not spread throughout the cluster. This allows for the possibility of clusters possessing nonzero dipole moments. We have also done simulations with conductive monomers, where charges can be neutralized on aggregation. Of course, since conductive clusters can contain only one sign of residual charge, no cluster dipole moments are possible. For these clusters, the residual charge gets spread among the monomers one unit charge at a time in such a way as to minimize the coulomb energy within the cluster.

Specifically, we were interested in seeing the effect of charging on growth kinetics, morphologies, and size distributions. As far as kinetics is concerned, the low charge percentage (less than 10% of the monomers being charged) used in our simulations does not yield significant differences in the growth of clusters.

In studies of carbon soot in ethylene/air laminar diffusion flames Maricq found that the charge distributions broaden as the aggregation proceeds. We observe this in our simulations. However, it does not appear that the charges are significantly influencing the aggregation process, as similar results are obtained when we turn the charge interactions off and simply label the “charged” monomers. The results indicate that charged monomers are simply getting statistically placed in clusters upon aggregation the same as any other monomer. This may not be true of systems where the initial population of charged particles is higher, and this is something we are continuing to investigate.

To continue our study of charged aggregation a number of things are being done simultaneously. First, as already mentioned, the aggregation of charged systems with a higher initial percentage of charges is being investigated both in the case of bipolar and unipolar charging. To better understand the results in the Epstein regime, a comparison of the aggregation of uncharged monomers using both possibilities for diffusion constant ( $R_g^{-2}$  and  $A^{-1}$ ) is being done and a comparison made to the expectations from scaling theory. Finally we are developing a Molecular Dynamics program to more correctly model the effect of the coulomb force, gravitational settling, etc.

# Light Scattering

## Mie Scattering

We continued our previous studies of patterns in Mie scattering. Our tactic to use as an alternative to the traditional scattering angle  $\theta$  in describing light scattering from a uniform dielectric sphere; that alternative is the dimensionless parameter  $qR$ , where  $R$  is the radius of the sphere,  $q = 2k \sin(\theta/2)$  and  $k$  is the wave number of the incident light. Simple patterns appear in the scattered intensity if  $qR$  is used in place of  $\theta$  that have not been previously recognized (fig. 14). These patterns are characterized by the envelopes approximating the scattered intensity distributions and are quantified by the phase shift parameter  $\rho = 2kR|m-1|$  where  $m$  is the real refractive index of the sphere. We found new patterns in these envelopes when the scattered intensity is normalized to the Rayleigh differential cross section. Mie scattering is similar to Rayleigh scattering when  $\rho < 1$  and follows simple patterns for  $\rho > 1$  which evolve predictably as a function of  $\rho$ . The curves have a semi-quantitative universality with  $\rho$ . These patterns allow us to present a unifying picture of the evolution of Mie scattering for changes in  $kR$  and  $m$  (fig. 15).

## Multiple Scattering

We showed that the extent and effect of multiple scattering on angularly resolved light-scattering intensity measurements, the optical structure factor, can be quantitatively described by a single parameter, the average number of scattering events along the scattering volume. This quantity is easily measured or calculated and hence provides a useful experimental indicator of multiple scattering, which is a hindrance to accurate structure factor measurements.

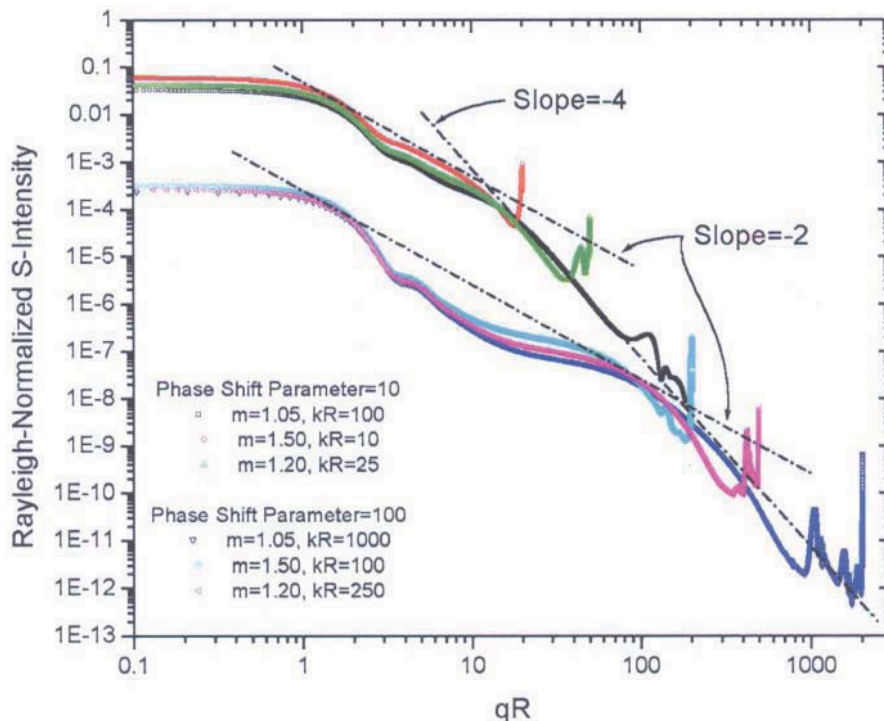


Figure 14.—Scattered light intensity normalized by the Rayleigh cross section for spheres of arbitrary radius  $R$  and refractive index  $m$  versus  $qR$ . Note quasi universality on the shift parameter  $\rho = 2kR|m-1|$ .

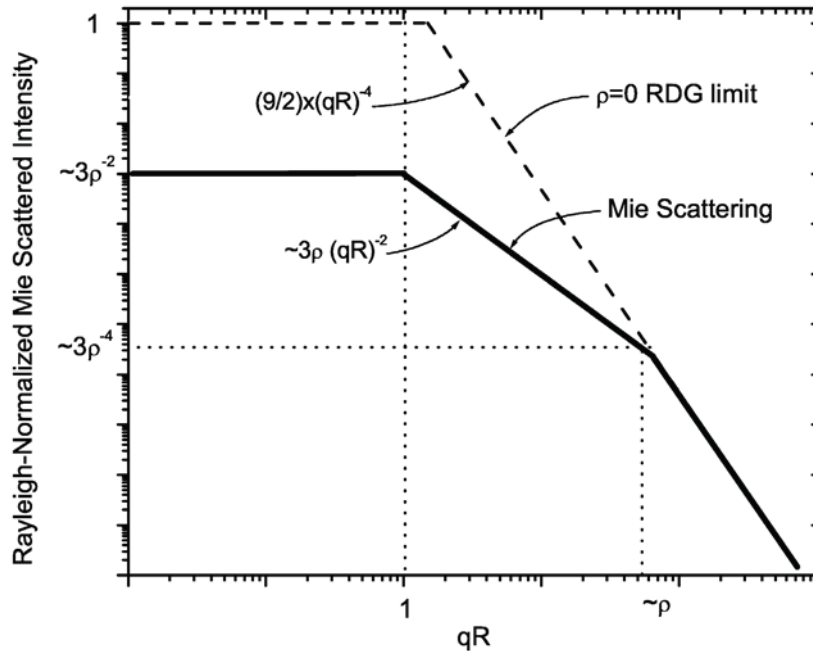


Figure 15.—Schematic of Mie scattering behavior.

## References

### Papers Published Under NASA Support

1. “Enhanced Kinetics and Free-Volume Universality in Dense Aggregating Systems,” D. Fry, T. Sintes, A. Chakrabarti, and C.M. Sorensen, *Phys. Rev. Lett.* **89**, 148301 (2002).
2. “Observation of Soot Superaggregates With a Fractal Dimension of 2.6 in Laminar Acetylene/Air Diffusion Flames,” C.M. Sorensen, W. Kim, D. Fry, A. Chakrabarti, *Langmuir* **19**, 7560–7563 (2003).
3. “Universal Occurrence of Soot Aggregates with a Fractal Dimension of 2.6 in Heavily Sooting Laminar Diffusion Flames,” W. Kim, C.M. Sorensen, A. Chakrabarti, *Langmuir* **20**, 3969–3973 (2004).
4. “Structural Crossover in Dense Irreversibly Aggregating Particulate Systems,” D. Fry, A. Chakrabarti, W. Kim, C.M. Sorensen, *Phys. Rev. E* **69**, 061401–10 (2004).
5. “Computer Simulation of Selective Aggregation in Binary Colloids,” F. Pierce, A. Chakrabarti, D. Fry, and C.M. Sorensen, *Langmuir* **20**, 2498–2502 (2004).
6. “Kinetics of Phase Transformations in Depletion-Driven Colloids,” J.J. Cerda, Tomas Sintes, C.M. Sorensen, and A. Chakrabarti, *Phys. Rev. E* **70**, 011405 (2004).
7. “Molecular Dynamics Simulation of the Transition from Dispersed to Solid Phase,” A. Chakrabarti, D. Fry and C.M. Sorensen, *Phys. Rev. E* **69**, 031408 (2004).
8. “Structure Factor Scaling in Colloidal Phase Separation,” J.J. Cerda, T. Sintes, C.M. Sorensen and A. Chakrabarti, *Phys. Rev. E* **70**, 051405 (2004).
9. “Aggregation-Fragmentation in a Model of DNA-Mediated Colloidal Assembly,” F. Pierce, C.M. Sorensen, A. Chakrabarti, *Langmuir* **21**, 8992–8999 (2005).
10. “Multiple Scattering Effects on Optical Structure Factor Measurements,” T. Mokhtari, C.M. Sorensen and A. Chakrabarti, *Applied Optics* **44**, 7858 (2005).
11. “Patterns in Mie Scattering: Evolution when Normalized by the Rayleigh Cross Section,” M.J. Berg, C.M. Sorensen, and A. Chakrabarti, *Applied Optics* **44**, 7487–7493 (2005).

12. “Hybrid Superaggregate Morphology as a Result of Aggregation in a Cluster Dense Aerosol,” R. Dhaubhadel, F. Pierce, A. Chakrabarti, and C.M. Sorensen, *Phys. Rev. E* **73**, 011404 (2006).
13. “Soot Aggregates, Superaggregates and Gel-Like Networks in Laminar Diffusion Flames,” W.G. Kim, C.M. Sorensen, D. Fry and Amit Chakrabarti, *J. Aerosol Science* **37**, 386 (2006).
14. “Computer Simulation of Diffusion-Limited Cluster-Cluster Aggregation with an Epstein Drag Force,” F. Pierce, C.M. Sorensen, and A. Chakrabarti, *Phys. Rev. E* **74**, 021411 (2006).
15. “Aerosol Gelation: Synthesis of a Novel, Lightweight, High Specific Surface Area Material,” R. Dhaubhadel, G. Gerving, A. Chakrabarti and C.M. Sorensen, *Aerosol Sci. Tech.* **41**, 804–810 (2007).

### **Patent**

Creation of Ultralow Density Porous Materials via Aerosol Gelation: Aerosol Gels, patent pending.

### **Theses**

- Dan Shi, MS, 2001, “Experimental Studies of the Optical Structure Factor of Soot Clusters in a Heavily Sooting Acetylene Flame.”
- Dan Fry, Ph.D., 2003, “Aggregation in Dense Particulate Systems.”
- Corey Gerving, MS, 2004, “Production of Low Density Aero-Gels Through the Controlled Detonation of Hydrocarbon Fuels.”
- Flint Pierce, Ph.D. 2007, “Aggregation in Aerosols and Colloids.”
- Matthew Berg, Ph.D. (expected) 2008, “Light Scattering.”
- Rajan Dhaubhadel, Ph.D. (expected) 2008, “Aerosol Gelation.”

**REPORT DOCUMENTATION PAGE**

*Form Approved*  
OMB No. 0704-0188

The public reporting burden for this collection of information is estimated to average 1 hour per response, including the time for reviewing instructions, searching existing data sources, gathering and maintaining the data needed, and completing and reviewing the collection of information. Send comments regarding this burden estimate or any other aspect of this collection of information, including suggestions for reducing this burden, to Department of Defense, Washington Headquarters Services, Directorate for Information Operations and Reports (0704-0188), 1215 Jefferson Davis Highway, Suite 1204, Arlington, VA 22202-4302. Respondents should be aware that notwithstanding any other provision of law, no person shall be subject to any penalty for failing to comply with a collection of information if it does not display a currently valid OMB control number.

PLEASE DO NOT RETURN YOUR FORM TO THE ABOVE ADDRESS.

<b>1. REPORT DATE (DD-MM-YYYY)</b> 01-08-2008		<b>2. REPORT TYPE</b> Final Contractor Report		<b>3. DATES COVERED (From - To)</b>	
<b>4. TITLE AND SUBTITLE</b> Gelation in Aerosols: Non-Mean-Field Aggregation and Kinetics				<b>5a. CONTRACT NUMBER</b>	
				<b>5b. GRANT NUMBER</b> NAG3-2360; NNC04GA746	
				<b>5c. PROGRAM ELEMENT NUMBER</b>	
<b>6. AUTHOR(S)</b> Sorensen, C., M.; Chakrabarti, A.				<b>5d. PROJECT NUMBER</b>	
				<b>5e. TASK NUMBER</b>	
				<b>5f. WORK UNIT NUMBER</b> WBS 095240.04.03.03.02.04	
<b>7. PERFORMING ORGANIZATION NAME(S) AND ADDRESS(ES)</b> Department of Physics Cardwell Hall Kansas State University Manhattan, Kansas 66506-2601				<b>8. PERFORMING ORGANIZATION REPORT NUMBER</b> E-16546	
<b>9. SPONSORING/MONITORING AGENCY NAME(S) AND ADDRESS(ES)</b> National Aeronautics and Space Administration Washington, DC 20546-0001				<b>10. SPONSORING/MONITORS ACRONYM(S)</b> NASA	
				<b>11. SPONSORING/MONITORING REPORT NUMBER</b> NASA/CR-2008-215280	
<b>12. DISTRIBUTION/AVAILABILITY STATEMENT</b> Unclassified-Unlimited Subject Categories: 70 and 25 Available electronically at <a href="http://gltrs.grc.nasa.gov">http://gltrs.grc.nasa.gov</a> This publication is available from the NASA Center for AeroSpace Information, 301-621-0390					
<b>13. SUPPLEMENTARY NOTES</b>					
<b>14. ABSTRACT</b> Nature has many examples of systems of particles suspended in a fluid phase; colloids when in a liquid, aerosols when in a gas. These systems are inherently unstable since if the particles can come together, van der Waals forces will keep them together. In this work we studied the aggregation kinetics of particulate systems, most often aerosols. The emphasis of our work was to study dense systems and systems that gel since previous work had not considered these. Our work obtained a number of significant discoveries and results which are reported here.					
<b>15. SUBJECT TERMS</b> Aerosols; Gels; Colloids; Fractals; Nanoparticles; Soot					
<b>16. SECURITY CLASSIFICATION OF:</b>			<b>17. LIMITATION OF ABSTRACT</b>	<b>18. NUMBER OF PAGES</b>	<b>19a. NAME OF RESPONSIBLE PERSON</b>
<b>a. REPORT</b>	<b>b. ABSTRACT</b>	<b>c. THIS PAGE</b>			<b>19b. TELEPHONE NUMBER (include area code)</b>
U	U	U	UU	19	STI Help Desk (email:help@sti.nasa.gov) 301-621-0390



